

Intrinsic strangeness and charm of the nucleon using improved staggered fermionsW. Freeman^{1,*} and D. Toussaint^{2,†}

(MILC Collaboration)

¹*Department of Physics, George Washington University, 725 21st Street Northwest, Washington, DC 20052, USA*²*Department of Physics, University of Arizona, 1118 East 4th Street, Tucson, Arizona 85721, USA*

(Received 19 April 2012; published 9 September 2013)

We calculate the intrinsic strangeness of the nucleon, $\langle N|\bar{s}s|N\rangle - \langle 0|\bar{s}s|0\rangle$, using the MILC library of improved staggered gauge configurations using the Asqtad and HISQ actions. Additionally, we present a preliminary calculation of the intrinsic charm of the nucleon using the HISQ action with dynamical charm. The calculation is done with a method which incorporates features of both commonly used methods, the direct evaluation of the three-point function and the application of the Feynman-Hellman theorem. We present an improvement on this method that further reduces the statistical error, and check the result from this hybrid method against the other two methods and find that they are consistent. The values for $\langle N|\bar{s}s|N\rangle$ and $\langle N|\bar{c}c|N\rangle$ found here, together with perturbative results for heavy quarks, show that dark matter scattering through Higgs-like exchange receives roughly equal contributions from all heavy quark flavors.

DOI: [10.1103/PhysRevD.88.054503](https://doi.org/10.1103/PhysRevD.88.054503)

PACS numbers: 12.38.Gc, 14.20.Dh

I. INTRODUCTION

The intrinsic strangeness of the nucleon, the matrix element $\langle N|\int d^3x\bar{s}s|N\rangle - \langle 0|\int d^3x\bar{s}s|0\rangle$ (often abbreviated $\langle N|\bar{s}s|N\rangle$, with the vacuum subtraction and volume integral omitted), has been a quantity of significant interest in the past few years due to its relevance to weakly interacting massive particles(WIMP)-on-nucleon scattering cross sections in many models [1,2]. This scattering process is shown in Fig. 1. Early χ PT calculations suggested that its value might be quite large [3]. Early lattice calculations of its value suffered from large statistical errors and/or uncontrolled systematic effects [4–8], and the results are somewhat inconsistent. More recently, there have been a number of more modern calculations with better control of systematic errors, notably the use of fermion actions retaining all or part of the continuum chiral symmetries, which are roughly in agreement [9–21], including earlier work by us [22] which is extended here. Figure 2 shows a graphical depiction of the history of calculations, mostly using lattice QCD, of the matrix element $\langle N|\bar{s}s|N\rangle$.

We present a refinement of this method, originally discussed in Ref. [27], which reduces statistical error while requiring, in principle, no additional computational effort. However, due to averaging of propagators and condensate measurements done by MILC in their original Asqtad analysis, application of this method requires recomputation of propagators and the quark condensate. We thus only use the refined technique on a subgroup of the available Asqtad ensembles. Applying these methods to the MILC Asqtad

data [28] to calculate $\langle N|\bar{s}s|N\rangle$, we obtain results very similar to those in Ref. [22], but with smaller statistical and systematic errors.

We also perform a direct evaluation of $\langle N|\bar{s}s|N\rangle$ on those Asqtad ensembles where the propagators and condensate measurements have been rerun. This technique, while inferior on the MILC data set, has been used by a number of other calculations, for instance [11,12], and is more theoretically straightforward; thus, it provides a useful cross-check with our “hybrid method” for $\langle N|\bar{s}s|N\rangle$. The results from these methods are in excellent agreement.

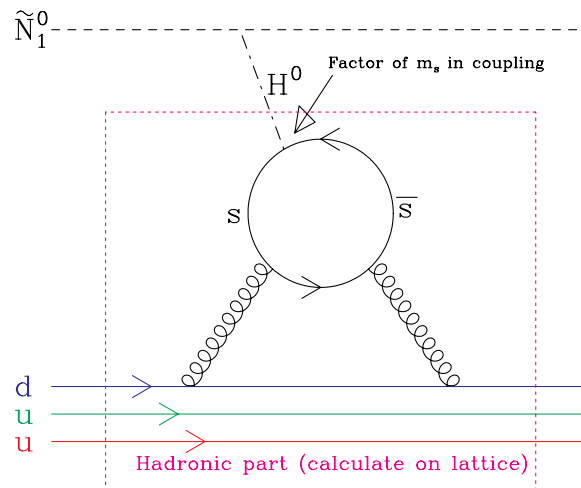


FIG. 1 (color online). Feynman diagram of an incoming neutralino interacting with a sea strange quark loop in the proton, mediated by a Higgs boson. The overall interaction amplitude depends on the intrinsic strangeness of the nucleon which must be computed on the lattice.

*wfreeman@gwu.edu

†doug@physics.arizona.edu

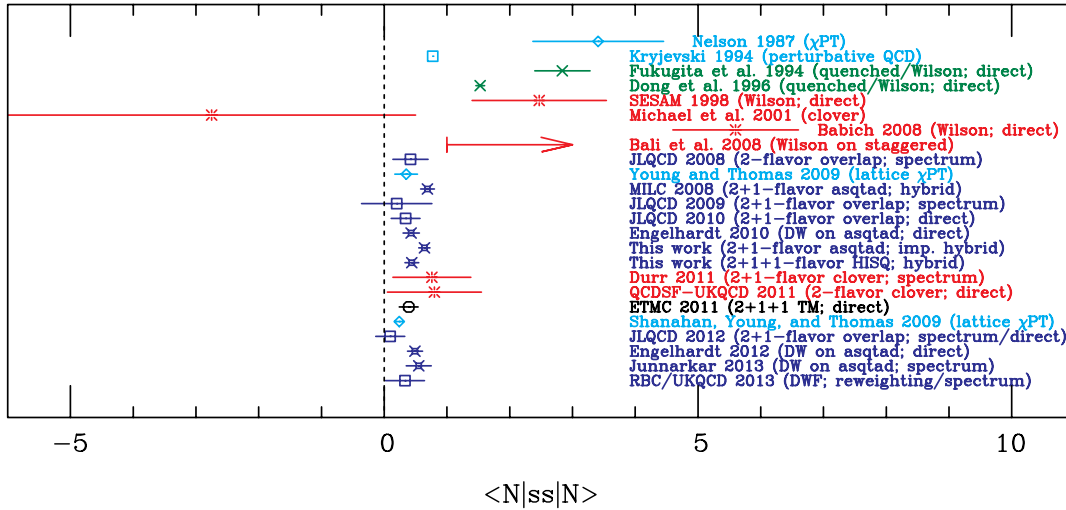


FIG. 2 (color online). A history of calculations of the nucleon strangeness. The “natural scale”, given by the perturbative QCD calculation [23] as discussed in II A, is shown as a vertical blue dashed line [3–10,12–14,16–26].

We also apply this method to the newer HISQ gauge configurations to calculate both $\langle N|\bar{s}s|N\rangle$ and $\langle N|\bar{c}c|N\rangle$. The result for the intrinsic strangeness is somewhat lower on the HISQ data, although it is not wildly different; the result for the intrinsic charm has large errors but is consistent with a perturbative prediction.

II. THE MEANING OF THE “NUCLEON STRANGENESS”

The term “intrinsic strangeness of the nucleon” for this matrix element is somewhat deceptive. While in perturbation theory the relevant diagram involves a sea strange quark loop (see Fig. 1), this does not imply that the presence of the valence light quarks in the nucleon somehow elicits strange quark loops from the vacuum where none would exist otherwise. In fact, the meaning of the nucleon strangeness is almost exactly the opposite of this. The vacuum strange quark loops, as part of the strange quark chiral condensate, pervade all space; the presence of the valence quarks, in fact, partially *suppresses* the natural vacuum condensate. The “strangeness of the nucleon” is really the suppression of this vacuum behavior.

Chiral symmetry for the strange quark is only an approximate symmetry; it is broken explicitly by the mass term $m_s\bar{s}s$ in the QCD Lagrangian. This explicit breaking determines the direction of the spontaneous breaking of chiral symmetry; the symmetry is broken in the direction that minimizes the action, leading to a negative expectation value for $\bar{s}s$ in the QCD vacuum, with the usual sign convention that the mass term in the Euclidean Lagrangian is $+m_s\bar{s}s$. In the presence of the valence quarks in the nucleon, the magnitude of the condensate is reduced. Since the “strangeness of the nucleon” is defined as $\langle N|\bar{s}s|N\rangle - \langle 0|\bar{s}s|0\rangle$, its natural sign is positive: both terms are negative in sign, but the vacuum term is larger in

magnitude. A schematic depiction of the nucleon’s “bubble” in the vacuum strange quark condensate is shown in Fig. 3. The probability for an incident WIMP to scatter off of this bubble can be understood in the same way as light scattering off of a bubble in a piece of glass: it is the change in the properties of the medium, not the absolute presence or absence of those properties, that causes the scattering.

A. Perturbative predictions

The nucleon strangeness is an inherently nonperturbative quantity, since the strange quark is too light to be

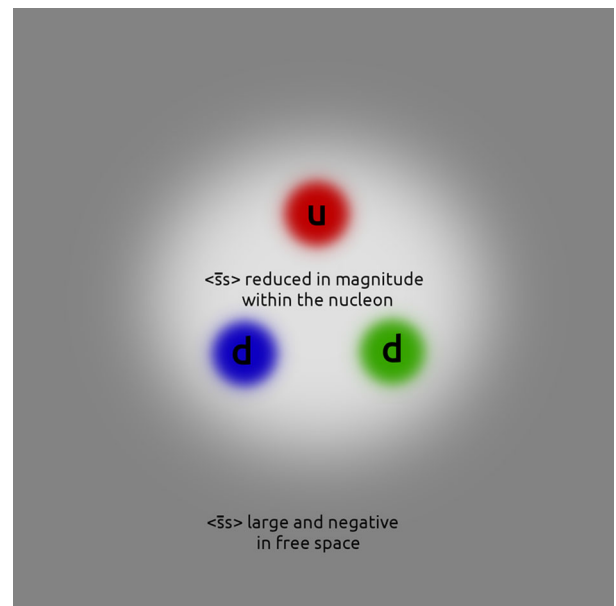


FIG. 3 (color online). A schematic illustration of the strangeness of the nucleon: the presence of the valence quarks creates a “bubble” in the vacuum chiral condensate.

treated properly in perturbation theory. For sufficiently heavy quarks, however, there is a perturbative approach to calculate the $\langle N|\bar{q}q|N\rangle - \langle 0|\bar{q}q|0\rangle$ matrix element. This calculation is enlightening in two ways. First, it allows for a theoretical calculation of the intrinsic charm of the nucleon. The intrinsic charm is similar in character to the intrinsic strangeness, and can be calculated on the lattice in the same ways. This allows contact with the lattice result for the intrinsic charm. Second, while there is no reason to expect it to be correct for the strange quark, the perturbative result nonetheless sets a natural scale for the nucleon strangeness. As we shall see, the value of $m_q\langle N|\bar{q}q|N\rangle$ is roughly constant for (perturbatively) heavy quarks. Lattice simulation must determine if the nucleon strangeness is substantially enhanced above this natural scale (as suggested in Ref. [3] and some early lattice studies) or not.

Beginning with work of Shifman, Vainstein and Zakharov [29] and continuing through a four-loop perturbation theory calculation by Kryjevski [23], the scalar condensate of a heavy quark in the nucleon is

$$\frac{m_q}{M_N}\langle N|\bar{q}q|N\rangle = \frac{2}{33 - 2n_l}\{1 + C_1\alpha_s \dots\}, \quad (1)$$

where n_l is the number of quark flavors lighter than the heavy quark. (The explicit perturbative corrections may be found in Ref. [23].)

The important point is that when a heavy quark mass $m_q \gg \Lambda$, M_N is varied, with the bare coupling constant held fixed, the nucleon mass is affected in the same manner as the scale Λ at which α_Λ runs to a particular value. Since the running of the coupling constant sets the scale for hadronic physics with light quarks, this amounts to saying that varying a heavy quark mass has no effect on the physical value of M_N or of any other low-energy lattice observable; rather, it amounts to an overall change in lattice scale setting. (Recall that the quantity M_N appearing in the Feynman-Hellman relation $\frac{\partial M_N}{\partial m_q} = \langle N|\bar{q}q|N\rangle$ is the lattice nucleon mass, not a nucleon mass in physical units, since the latter quantity is ambiguous and depends on the method used to set the lattice scale: one could choose M_N itself as the benchmark quantity to use in lattice scale-setting, giving $\frac{\partial M_N}{\partial m_q} \equiv 0$ under all circumstances!)

Thus, $\frac{\partial M_N}{\partial m_q}$ depends on the running of the coupling constant from its bare value α_0 at scale μ_0 to its value α_Λ . At one-loop order, where the dependence of g^{-2} on $\log \mu$ depends only on the number of light quark flavors, changing the charm quark mass from m_c to m'_c only changes the scale at which the charm quark freezes out from the beta function, and the low-mass limit of $\frac{\partial M_N}{\partial m_c}$ can be calculated simply.

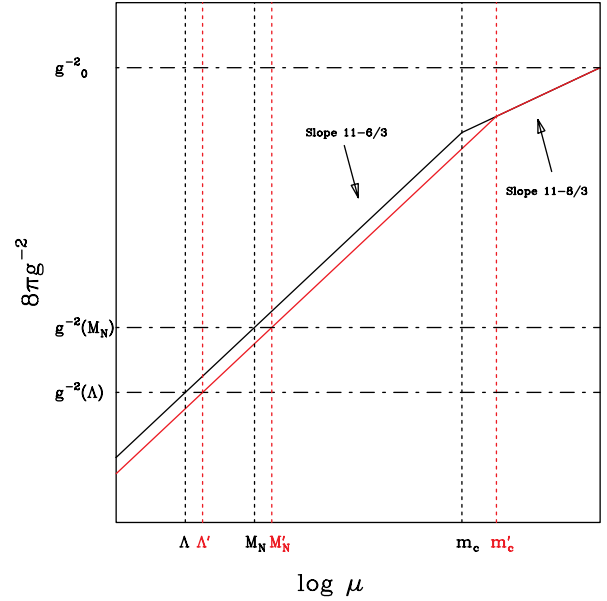


FIG. 4 (color online). A schematic depiction of the perturbative approach to $\frac{\partial M_N}{\partial m_c}$ taken by Shifman and Kryjevski at leading order, inspired by a similar presentation by Kryjevski in Ref. [23]. Changing the mass of a heavy quark changes the scale at which it freezes out and thus affects the running of the coupling constant, affecting all low-mass scales equally.

(This is true for any other flavor of heavy quark equally, of course.) This approach is shown graphically in Fig. 4.

While we would not trust a perturbative calculation at the strange quark mass, Eq. (1) defines a natural scale for quark condensates, and lattice calculations are needed to see if the strange quark content is in fact enhanced relative to this scale.

III. METHODS

A. The direct method

A theoretically straightforward, but practically difficult, way to evaluate the nucleon strangeness is to just evaluate the needed matrix element directly. One computes

$$\langle N|\bar{s}s|N\rangle = \frac{\langle N^\dagger(0)N(T)\bar{s}s(T_1)\rangle}{\langle N^\dagger(0)N(T)\rangle} - \langle \bar{s}s \rangle, \quad (2)$$

where T is the source-sink separation of the nucleon propagator, and T_1 is an intermediate time chosen sufficiently far from both 0 and T that the overlap with the excited states is small. (Here again volume integrals have been omitted.)

In the limit where $e^{-M_N n_t} \ll 1$ (i.e. states wrapping around the lattice are irrelevant), this can be written as

$$\langle N|\bar{s}s|N\rangle = \frac{\sum N^\dagger(T_0)N(T_0+T)\bar{s}s(T_0+T_1) + N^\dagger(T_0)N(T_0-T)(-1)^T\bar{s}s(T_0-T_1)}{\sum N^\dagger(T_0)N(T_0+T) + N^\dagger(T_0)N(T_0-T)(-1)^T} - \sum_{\text{configs}} \frac{1}{n_t} \sum_t \bar{s}s(t), \quad (3)$$

where T_0 are the source locations of the nucleon propagators, T is their length, T_1 is an intermediate length at which the strange quark condensate is measured, and the sums run over all gauge configurations and all source locations on each configuration. The factor of $(-1)^T$ comes from the fact that a backward-propagating nucleon state in the staggered fermion formulation carries this factor.

This approach requires the evaluation of $N^\dagger(0)N(T)$ at appropriate distances T , along with the evaluation of the strange quark condensate $\int d^3x \bar{s}s(x, t)$ on intermediate time slice(s) T_1 . This is not part of the standard MILC analysis program, which only records $N^\dagger(0)N(T)$ averaged over all source time slices (typically 8 per configuration), and only records the whole-lattice condensate $\int d^4x \bar{s}s(x, t)$ rather than separate values per time slice. Thus, without extra computer work to recompute correlators and condensates, this method cannot be used on the MILC results.

B. The spectrum method

An alternate route to $\langle N|\bar{s}s|N\rangle$ involves the Feynman-Hellman theorem, to equate $\langle N|\bar{s}s|N\rangle$ with $\frac{\partial M_N}{\partial m_s}$. This relation may be derived by differentiating the partition function with respect to m_s and using the fact that $\langle N^\dagger(0)N(T)\rangle = e^{-M_N T}$ for an ideal nucleon operator. This method has the disadvantage that it requires multiple ensembles with different values of m_s but all other lattice parameters held fixed, a condition not met by the existing MILC data.

C. The hybrid method

The two traditional methods for calculating the nucleon strangeness would be expensive for the MILC ensembles: the direct method would require recomputation of propagators, while the spectrum method would require different ensemble parameters. Thus, we use a third method, originally presented in Ref. [22], which combines their advantages: it can obtain a value for $\langle N|\bar{s}s|N\rangle$ from a single lattice ensemble with arbitrary lattice parameters, using only the whole-lattice average condensate and correlators averaged over all source time slices that are available.

The nucleon mass M_N is obtained by a fit to the nucleon propagator $P(t)$ and as such can be thought of as a complicated function of the propagator at different times: $M_N = f(P(t_1), P(t_2), P(t_3) \dots)$. The crucial idea is that one can use the chain rule for differentiation to rewrite the derivative:

$$\frac{\partial M_N}{\partial m_s} = \frac{\partial M_N}{\partial P(t_1)} \frac{\partial P(t_1)}{\partial m_s} + \frac{\partial M_N}{\partial P(t_2)} \frac{\partial P(t_2)}{\partial m_s} + \dots \quad (4)$$

The partial derivatives $\frac{\partial M_N}{\partial P(t_i)}$ can be evaluated most simply by applying a small perturbation to the nucleon propagator and examining the change in the fit result, while the second partial derivative $\frac{\partial^2 P(t_i)}{\partial m_s^2}$ can be evaluated by an

application of the Feynman-Hellman theorem in reverse to relate it to $\langle P(t_i)\bar{s}s\rangle - \langle P(t_i)\rangle\langle\bar{s}s\rangle$.

The measurements of $\bar{s}s$ have been made using the commonly used stochastic estimator technique. Typically, MILC has made such measurements as part of lattice generation to monitor equilibration and simulation-time autocorrelations and to use for subtracting zero temperature values in equation of state calculations. On most ensembles, enough estimates are available that the fluctuation of the stochastic estimator is a small part of the overall uncertainty. On a few of the coarsest ($a \approx 0.12$ fm) ensembles, we have run additional estimates of $\bar{s}s$ to ensure that the stochastic estimator does not introduce any meaningful error. While other groups have found it expedient to project out the low modes of the Dirac operator and calculate their contribution exactly, we find that using these configurations it is sufficiently cheap and precise to simply use repeated stochastic estimators on the entire space.

Prior results obtained by applying this method to the MILC Asqtad gauge configurations can be found in Ref. [22].

D. The improved hybrid method

In the original hybrid method, a major contribution to the statistical error in this calculation comes from fluctuations in the quark condensate that have no physical correlation with the hadron propagator. While the correlation between these fluctuations and the propagator averages to zero in the limit of infinite statistics, with finite statistics it does not, and spurious correlations of this sort are a major contributor to statistical error.

Since there is no physical reason that fluctuations in the quark condensate far from the propagator should be correlated with it, those fluctuations contribute only noise and can be discarded without introducing bias; in other words, we replace

$$\frac{\partial P(T)}{\partial m_s} = \left\langle P(T) \int d^3\vec{x} dt \bar{s}s(\vec{x}, t) \right\rangle - \left\langle P(T) \right\rangle \left\langle \int d^3\vec{x} dt \bar{s}s(\vec{x}, t) \right\rangle \quad (5)$$

with

$$\frac{\partial P(T)}{\partial m_s} = \left\langle P(T) \int d^3\vec{x} \int_{t_1}^{t_2} dt \bar{s}s(\vec{x}, t) \right\rangle - \left\langle P(T) \right\rangle \left\langle \int d^3\vec{x} \int_{t_1}^{t_2} dt \bar{s}s(\vec{x}, t) \right\rangle \quad (6)$$

where t_1 and t_2 are chosen sufficiently far from the propagation region so that they do not affect the final result.

The application of this method to the MILC Asqtad ensembles requires some extra computer time, since it requires separate values of $\bar{s}s$ on each time slice and of the nucleon propagator for each source location; these separate values were not saved originally due to a desire

to economize on storage. Due to the expense of this on the finest ensembles, we have only completed these measurements on the $a \approx 0.12$ fm Asqtad ensembles and some of the $a \approx 0.09$ fm Asqtad ensembles.

IV. $\langle N|\bar{s}s|N \rangle$ FROM THE MILC ASQTAD DATA

A. Validity tests of the improved hybrid method

The hybrid method is exact, but subject to the usual systematic errors that affect lattice calculations: pollution from excited states, finite size effects, and lattice discretization errors. The improved hybrid method, however, only considers the strange quark condensate on those time slices that are meaningfully correlated with the propagator, and is thus only valid if the correlation between the quark condensate and the propagator falls off reasonably rapidly away from the propagation region.

To test this assumption, it is useful to calculate the contribution of each time slice to the overall correlation between the propagator and the condensate, given by the expression

$$\left\langle P(T) \int d^3\vec{x} \bar{s}s(\vec{x}, t) \right\rangle - \langle P(T) \rangle \left\langle \int d^3\vec{x} \bar{s}s(\vec{x}, t) \right\rangle \quad (7)$$

(compare to Eq. (6)). This correlation is shown in Fig. 5.

These data show that the condensate is indeed only meaningfully correlated with the propagator within the propagation region and in a small window outside of it, confirming that this method is valid.

B. Choice of padding length

We must thus determine the appropriate size of the “padding” outside the propagation region in which condensate measurements will be considered. If this padding length is chosen to be too small, then the result will suffer from systematic error, as some of the physical correlations are not being considered; if it is chosen too large, then the result will be unnecessarily noisy and the full benefit from this method will not be realized.

Figure 5 suggests that the correlation between the condensate and the nucleon propagator outside a window consisting of the propagation region and a window of width $\sim 5a$ on either side is only noise. To see if only considering the condensate within this window improves the statistical error without introducing significant bias, we consider the resulting value of $\langle N|\bar{s}s|N \rangle$ and $\langle N|\bar{u}u|N \rangle$ for various widths of this padding on an average of the $a \approx 0.12$ fm ensembles. We use the same choice of the minimum fit distance $T_{\min} = 5a$ as in Ref. [22]. The result is shown in Fig. 6. All errors have been determined by either omit-10 or omit-20 jackknife; testing indicated no meaningful dependence of error estimates on which jackknife blocksize was used.

The salient feature of these graphs is the desired one: a substantial reduction in statistical error provided by the improved hybrid method. As expected, discarding physically unmeaningful condensate measurements which contribute only noise reduces the error bars by quite a bit.

Another notable feature is the difference between the results obtained from the old and new data on the same ensemble using the unimproved method (the fancy square

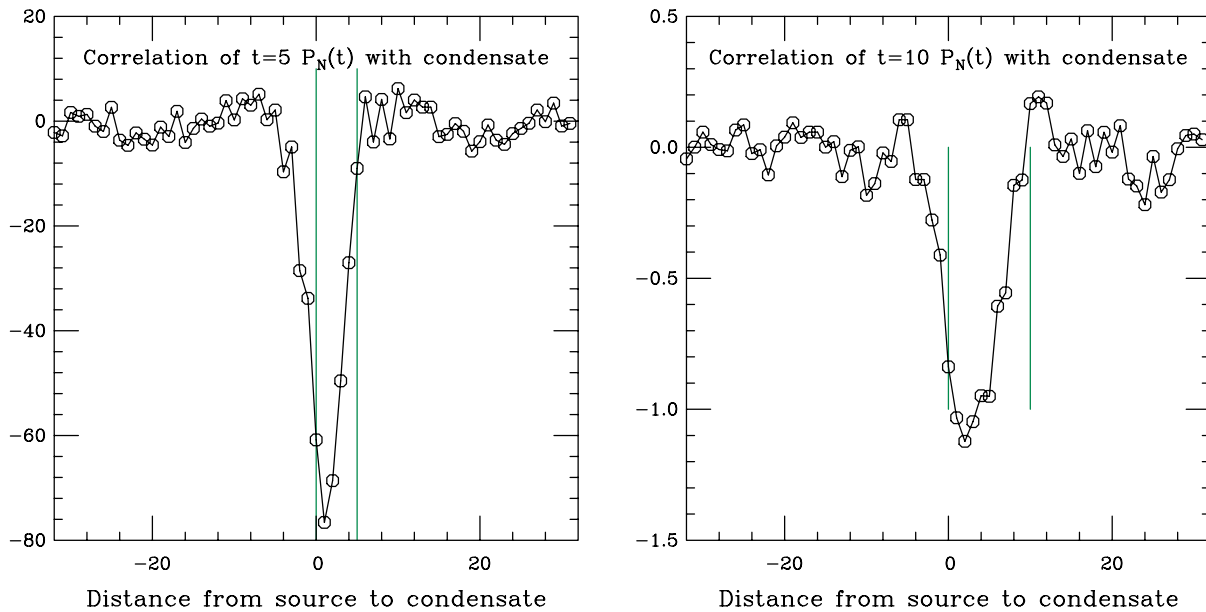


FIG. 5 (color online). The correlation between nucleon propagators of length $5a$, $10a$, and $15a$ with the strange quark condensate as a function of the distance from the propagator source on one of the MILC $a = 0.12$ fm ensembles. The source and sink location of the propagators are marked as green vertical lines.

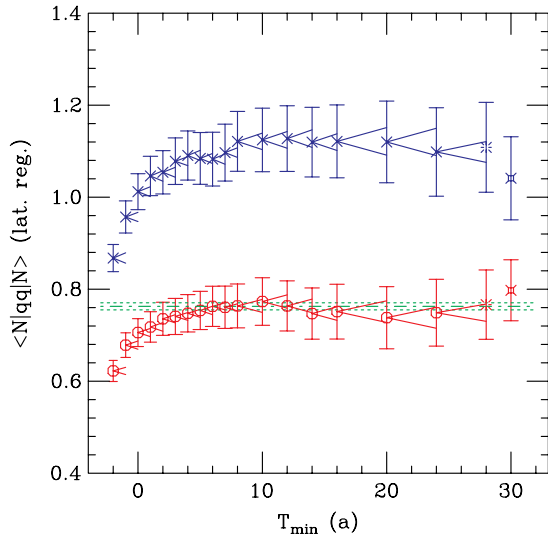


FIG. 6 (color online). Results for $\langle N|\bar{q}q|N \rangle$ using the improved hybrid method averaged over the $a \approx 0.12$ fm ensembles on which the needed measurements are available in the lattice regularization. Each graph shows the values of $\langle N|\bar{s}s|N \rangle$ (red circles) and $\langle N|\bar{u}u|N \rangle$ (blue crosses) at varying pad sizes. Negative pad sizes, with significant systematic bias, are included to make the trend of this bias plain. The result using the unimproved method (i.e. the limit of large pad size) on the newly-computed condensate and propagator measurements is shown as a starburst; the result using the unimproved method on the old data is shown as a fancy square for comparison. Note that the new data use different random time sources for the nucleon correlator. The uncertainty in the difference between adjacent values is shown as a horizontal carat centered on the left point; if the right point lies within the bracketed range then the difference between the two is less than one standard deviation. A horizontal band corresponding to the width of the systematic error estimate from the use of the improved method is shown.

and burst points, respectively). Part of this difference is due to the use of the stochastic estimator method to determine $\bar{s}s$. Indeed, by using the redone estimates of $\bar{s}s$ but the old propagators, we see some difference between the results. This effect, however, is not sufficient to explain the entire difference. The old and new propagators themselves are slightly different due to the use of different source time slices in the new data; when recomputing nucleon propagators, we used eight equally-spaced source time slices with the first located at a random offset from the lattice origin, which will not necessarily correspond to the eight sources used originally. This strongly suggests that the MILC practice of using only eight source time slices does not extract all available information about the nucleon propagator from the lattice, and that the statistical errors in M_N and $\langle N|\bar{s}s|N \rangle$ could be reduced further by the consideration of more source locations (requiring, of course, more inversions to compute the propagators).

Examining 6, we conclude that a conservative choice for padding size on the $a \approx 0.12$ fm ensembles is $6a$, while an

aggressive choice is $4a$. (The aggressive choice was made in [27]; here we present data with the conservative choice, which leads to essentially the same result but with slightly larger errors.) On the $a \approx 0.09$ fm ensemble, the equivalent padding size in physical units is $8a$. We estimate the systematic bias due to this procedure to be no more than 1%. This estimate is consistent with the result of fitting the data shown in 6 to constant-plus-exponential.

C. Minimum fit distance and excited state pollution

In Ref. [22], we chose minimum distances of $5a$, $7a$, and $10a$ on the $a = 0.12$, 0.09 , and 0.06 fm ensembles respectively, and gave a rather conservative estimate of the statistical error due to excited state pollution of 10%. These minimum distances, corresponding to a physical distance of ≈ 0.6 fm, were chosen to trade off statistical error (worse at higher minimum distances) and the possibility of bias due to excited-state contamination. The largest obstacle to determining the appropriate minimum distance T_{\min} and the excited-state systematic error estimate was the overall large statistical error in $\langle N|\bar{q}q|N \rangle$, making it difficult to tell the difference between systematic bias and statistical accident. It is possible that the improved statistical errors from the improved hybrid method may suggest a different choice of T_{\min} or a different estimate of the systematic error due to excited states.

The left pane of Fig. 7 shows the $\langle N|\bar{u}u|N \rangle$ and $\langle N|\bar{s}s|N \rangle$ matrix elements (in the lattice regularization) averaged over the five $a \approx 0.12$ ensembles on which the data for the improved method are available. We use the “aggressive” choice for padding size here ($4a$), on the grounds that a little bit of systematic error due to padding will not obscure trends in T_{\min} , and that the more aggressive choice may allow resolution of smaller systematic effects.

The difference between the average result on the coarse ensembles at $T_{\min} = 5$ and $T_{\min} = 6$ is about one standard deviation: this could be due either to systematic bias or simply a statistical fluctuation.

However, the difference is substantially smaller than 1σ on the $a \approx 0.09$ and $a \approx 0.06$ fm ensembles, suggesting that this 1σ difference is due to statistics rather than excited-state pollution. The right pane of Fig. 7 shows the dependence of $\langle N|\bar{u}u|N \rangle$ and $\langle N|\bar{s}s|N \rangle$ on T_{\min} for the $a \approx 0.09$ ensembles, in which no significant difference between $T_{\min} = 7$ (chosen as the optimum minimum distance) and $T_{\min} = 8$ is apparent. The more precise results available with the improved method, thus, are still consistent with the previous choices of T_{\min} . Note that the aim in the choice of T_{\min} is not to eliminate all systematic error from excited states, but to achieve a balance between statistical error (larger at higher T_{\min}) and systematic error (larger at lower T_{\min}). The absolute size of this difference is consistent with a 5% estimate for the systematic error due to excited states. Note that due to autocorrelations between the errors, an increasing trend is not necessarily

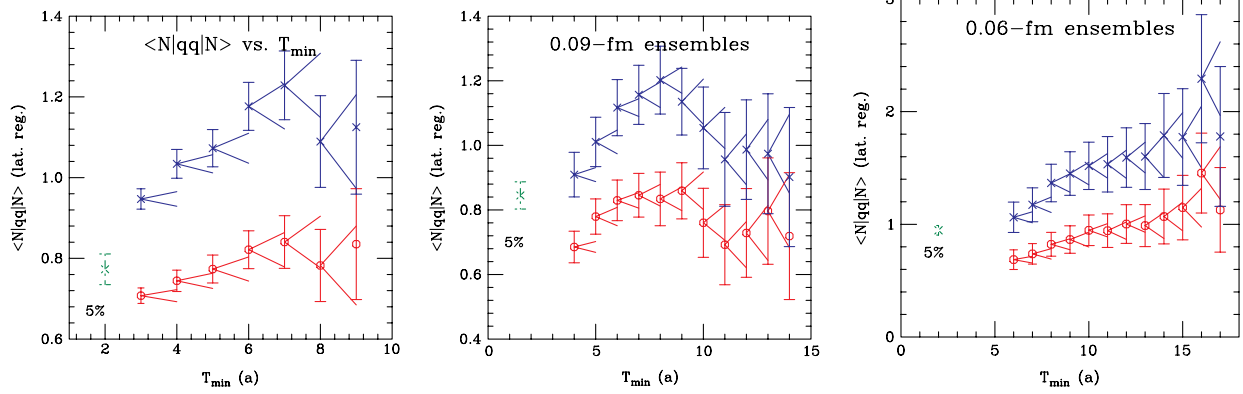


FIG. 7 (color online). $\langle N|\bar{u}u|N \rangle$ (blue crosses) and $\langle N|\bar{s}s|N \rangle$ (red circles) vs. T_{\min} using the (improved) hybrid method. The three panels show the average values on the 0.12 fm, 0.09 fm, and 0.06 fm ensembles, respectively; note the difference in the y-axis scale between the plots. The uncertainty in the difference between adjacent values (obtained by jackknife) is shown as a horizontal carat centered on the left point. The size of the 5% systematic error estimate from excited state pollution is shown with a green bar.

indicative of a systematic effect, and may just be a correlated statistical fluctuation in adjacent points.

This lower estimate for the systematic error due to excited states can also be justified by examining other information. The nucleon mass itself can be computed with much lower statistical error at higher T_{\min} ; mass fits at these higher minimum distances differ from those at $T_{\min} = 0.6$ fm by only 1% to 5%. Naïvely applying the perturbative argument to the nucleon strangeness, the quantity $\frac{m_s}{M_N} \langle N|\bar{s}s|N \rangle$ is the same for any hadron X , including the nucleon or the delta; thus, the fractional difference between the strangeness of the delta and the nucleon should be of the order of the fractional difference in their masses. We also note that in the quark model the nucleon and delta differ in the spin of the quarks, which we expect to be only indirectly related to the scalar strange quark content. Thus, we may expect the systematic error in $\frac{\partial M_N}{\partial m_s}$ due to excited state pollution to be smaller than the 1%–5% range for the systematic error in the nucleon mass. (The 1%–5% range does not imply that this systematic shift varies greatly from ensemble to ensemble; rather, at large T_{\min} M_N itself can only be determined to a few percent accuracy.)

It is possible to calculate a rough estimate of the fractional amount of excited-state pollution in a propagator of any given length using a nucleon propagator fitting method that includes the lowest-lying direct-parity excited state. (Note that due to the spin structure of staggered fermions, the nucleon interpolating operator used here overlaps in part with the delta, which is this lowest “excited state.”) These methods give results for the spectral weight and mass of the delta, allowing computation of the ratio $\frac{A_\Delta e^{-M_\Delta T}}{A_N e^{-M_N T}}$, the fractional amount of delta pollution, for any given propagator length T . For the chosen minimum distances, this ratio is generally less than 0.1. Since the nucleon-delta mass splitting is about 30%, and we expect the nucleon-delta strangeness difference to be not much

greater than 30%, this gives an estimate on the systematic shift due to delta pollution of 3%. While this is not a rigorous computation of the error due to finite-size effects, it does provide an independent estimate of its size without the high statistical error inherent in strangeness calculations and the associated difficulties in distinguishing between statistical fluctuations and systematic shifts.

D. Renormalization

The quantity $\frac{\partial M_N}{\partial m_s}$ is renormalization scheme and scale dependent, since m_s depends on the renormalization scheme and scale but M_N does not. Thus, as a first step in analysis we convert the results on each ensemble to a consistent renormalization scheme, such as $\overline{\text{MS}}$ (2 GeV). We used the Z-factors for converting from the Asqtad formulation to $\overline{\text{MS}}$ (2 GeV) which were calculated by the HPQCD Collaboration up to two-loop order in perturbation theory [30].

An alternative approach would be to work with the renormalization scheme dependent quantity $m_s \langle N|\bar{s}s|N \rangle$, or $F_{T_s} \equiv \frac{m_s}{M_N} \langle N|\bar{s}s|N \rangle$.

E. Chiral extrapolation

With one exception (with poor statistics), all of the MILC Asqtad gauge ensembles were performed with light quark masses significantly larger than the physical value of m_l . This necessitates an extrapolation of any lattice measurement to the physical light quark mass. Care must be taken in this extrapolation since the values of many quantities curve sharply very near the physical point, and a naïve polynomial extrapolation done on lattice data calculated with a typical range of light quark masses $m_l > 10$ MeV will miss this curvature.

The statistics in this study are not sufficiently strong to resolve subtle nonlinearities in the chiral form (or, equivalently, to determine higher-order low-energy

constants); they suffice only to do a linear extrapolation to the physical point. Thus, the presence of substantial curvature for low light quark mass (caused by $\frac{\partial^2 N}{\partial m_s \partial m_l}$ diverging as $m_l \rightarrow 0$ due to chiral logs) would cause substantial difficulties in the chiral extrapolation.

The mass of the nucleon in terms of the quark masses and (mostly unknown) χ PT coefficients has been calculated up to order m_q^2 in chiral perturbation theory [31], with the explicit form given in section IV of this reference. Differentiation with respect to m_s gives the chiral fit form for $\frac{\partial M_N}{\partial m_s}$. This form can then be examined for “dangerous” terms whose derivatives with respect to m_l diverge as $m_l \rightarrow 0$.

In this expansion there are no terms for which $\frac{\partial M_N}{\partial m_s}$ diverges as $m_l \rightarrow 0$. Another notable feature is the absence of a term $\approx m_s m_l \log(m_l)$. (This would be $\epsilon_{9,N}$ in the notation of Ref. [31], and would give a contribution to $\frac{\partial M_N}{\partial m_s} \sim m_l \log(m_l)$, formally larger than a correction linear in m_l .) (We thank Ulf Meissner for correspondence on this point.) Thus we can use a simple linear chiral extrapolation, of the form

$$\frac{\partial M_N}{\partial m_s} = A + B m_l. \quad (8)$$

F. Correcting for the strange quark mass

MILC tried to run most of the Asqtad ensembles at the physical value of the strange quark mass. However, since the lattice spacing is only determined *a posteriori* and since the physical strange quark mass itself is not trivial to measure, the Asqtad ensembles were run at nonphysical strange quark masses. Since the aim of this work is to calculate the strangeness of the nucleon for physical strange quarks, an adjustment is necessary. To correct for this and extrapolate the results to the physical value of m_s , we must determine the quantity $\frac{\partial}{\partial m_s} \langle N | \bar{s} s | N \rangle = \frac{\partial^2 M_N}{\partial m_s^2}$.

m_s has been most recently calculated by HPQCD on MILC lattices [30], and updated by MILC as part of a comprehensive fit of light meson masses and decay constants to chiral perturbation theory [32] as 89.0(0.2)(1.6) (4.5)(0.1) MeV in the $\overline{\text{MS}}$ (2 GeV) regularization scheme, where the errors are statistical, miscellaneous systematic, perturbative renormalization, and electromagnetic, respectively. For the purposes of this work we treat the value as 89 MeV exactly; the contribution of the uncertainty in m_s to the overall error in $\langle N | \bar{s} s | N \rangle$ is not significant, since m_s only enters this quantity indirectly. (Note that when we compute the RNG invariant $m_s \langle N | \bar{s} s | N \rangle$, where m_s appears directly, the uncertainty in m_s is very important.)

The values of m_s used in the MILC ensembles do not differ by enough to determine this quantity in any meaningful way by simply performing a fit. Thus, we must resort to a trick. The present method can also be used to calculate the equivalent light quark matrix element, equivalent to

$\frac{\partial M_N}{\partial m_{l,\text{sea}}}$, in exactly the same way. This quantity, interpreted as the amount that the nucleon suppresses the light quark condensate, has behavior qualitatively similar to the strangeness of the nucleon if m_l is sufficiently large that the strong enhancement near the chiral limit is not relevant; see Sec. IV E. On those MILC ensembles with the heaviest light quarks (for instance, where $m_l = 0.4 m_s$), we may treat the light sea quarks as “lighter strange quarks,” and write

$$\frac{\partial}{\partial m_s} \langle N | \bar{s} s | N \rangle = \frac{\langle N | \bar{s} s | N \rangle - \langle N | \bar{u} u | N \rangle}{m_s - m_l}. \quad (9)$$

This approach has the advantage that the numerator of the right-hand side is the difference of two correlated quantities, so the error on their difference (determined via the jackknife method, as usual) will be smaller than the naïve sum of their errors in quadrature.

We choose to apply this technique to all ensembles with $m_l \geq 0.15 m_s$. The results are shown in Table I. We use the improved hybrid method on the one of these ensembles where it is available. Fitting a constant to these results, we obtain

$$\frac{\partial}{\partial m_s} \langle N | \bar{s} s | N \rangle = -0.00331(28) \text{ MeV}^{-1}. \quad (10)$$

This value has been used to extrapolate measured values of $\langle N | \bar{s} s | N \rangle$ to the correct strange quark mass. The error on the slope of this extrapolation has been incorporated into the overall statistical error.

G. Continuum extrapolation

The leading-order discretization errors in the Asqtad action are $\mathcal{O}(a^2)$, so a continuum extrapolation can be

TABLE I. Results for $\frac{\langle N | \bar{s} s | N \rangle - \langle N | \bar{u} u | N \rangle}{m_s - m_l}$ on ensembles with heavy light quarks, presumed to be a good estimator of the dependence of the strangeness of the nucleon on strange quark mass, $\frac{\partial}{\partial m_s} \langle N | \bar{s} s | N \rangle$. The results are given in the $\overline{\text{MS}}$ (2 GeV) renormalization scheme. The result is also given for the $a \approx 0.12$ fm ensemble on which the improved method has been run. Errors are obtained via jackknife of the difference in the proper way. The result of fitting a constant to these values (using the improved method for the ensemble where it is available) is shown; this fit has $\chi^2/\text{d.o.f} = 7.76/4$.

β	a (nominal, fm)	$a m_l$	$a m_s$	$\frac{\partial}{\partial m_s} \langle N \bar{s} s N \rangle$ (MeV ⁻¹)
6.81	0.12	0.30	0.50	-0.0033(21)
6.79	0.12	0.20	0.50	-0.0021(6)
6.79	0.12	0.20	0.50	-0.0030(3) (improved)
7.10	0.09	0.093	0.31	-0.0067(19)
7.11	0.09	0.124	0.31	-0.0046(8)
7.48	0.06	0.72	0.18	-0.0046(24)
Average				-0.00331(28)

TABLE II. Discretization errors on other hadronic quantities on the Asqtad ensembles. The MILC collaboration has previously performed a well-constrained continuum extrapolation of each of these quantities; the discretization errors listed are the difference between the value at 0.12 fm and the continuum.

Quantity	0.12 fm discretization error
f_π, f_K , taste breaking	8.4%
f_π, f_K , other	2.6%
$r_1 M_N$	9.7%
$r_1 M_\rho$	7.2%

performed most simply by adding a term Ca^2 to the fit form used in the chiral extrapolation, and fitting to the form

$$\frac{\partial M_N}{\partial m_s} = A + Bm_l + Ca^2. \quad (11)$$

However, due to the large statistical error on $\langle N|\bar{s}s|N\rangle$ on the $a \approx 0.09$ fm and especially the $a \approx 0.06$ fm gauge ensembles compared to the likely discretization errors, it is difficult to perform a tightly constrained continuum extrapolation. Naïvely doing the fit given above gives a large uncertainty in C and thus a large uncertainty in the continuum limit.

However, the error band on the slope of the continuum extrapolation includes values which are highly unlikely, given our prior experience with continuum extrapolations of (more precisely measured) hadronic quantities on the Asqtad ensembles. The discretization errors in $\frac{\partial M_N}{\partial m_s}$ are likely broadly comparable to those in other similar hadronic quantities measured on the same gauge configurations; the size of these discretization errors are shown in Table II. We would be remiss not to take into account this information regarding the usual size of such discretization errors on the Asqtad ensembles, and the proper way to include these data is with a Bayesian prior. The most relevant of these other quantities is the nucleon mass; it also shows the largest discretization effect, so using it as the basis for a prior is both the most logical and the most conservative choice. We thus constrain C with a Bayesian prior centered on zero with a width corresponding to a shift in the nucleon strangeness of 10% from 0.12 fm to the continuum, taking into account our information about the usual size of discretization errors in hadronic quantities on the Asqtad lattices in as rigorous a way as possible.

H. Error budget and result

The value of $\langle N|\bar{s}s|N\rangle$ on each ensemble considered, along with the fit described in the preceding sections and its evaluation at the physical point, is shown in Fig. 8. While many included ensembles have large errors, the fit is controlled by a subset of ensembles with high statistics on which the data for the improved method are available. These ensembles are somewhat obscured in Fig. 8 by the lower-statistics ensembles with large errors; Fig. 9 shows

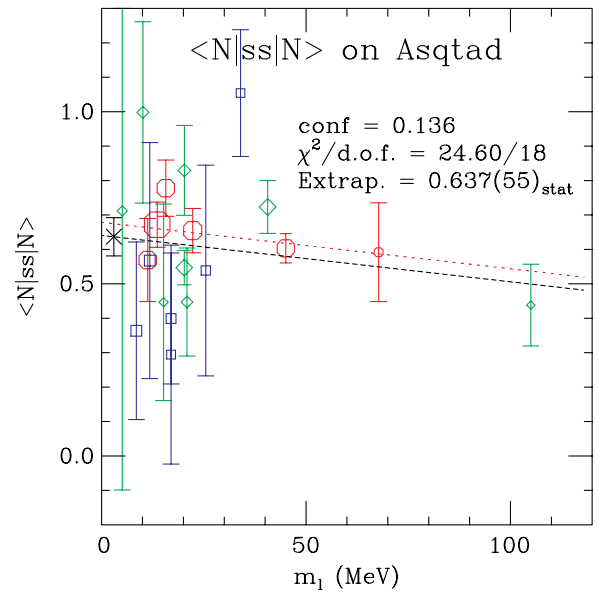


FIG. 8 (color online). $\langle N|\bar{s}s|N\rangle$ on the Asqtad ensembles using data from the improved hybrid method where it is available, in the $\overline{\text{MS}}$ (2 GeV) regularization scheme, adjusted to the correct value of m_s , along with the linear chiral and continuum fit. Data from the 0.12, 0.09, and 0.06 fm ensembles are shown by red octagons, green diamonds, and blue squares, respectively. The black line is the chiral fit in the continuum limit; the chiral fit at $a \approx 0.12$ fm is shown by the red dashed line. Symbol area is proportional to the number of lattices in the gauge ensemble. The black point marked by a cross is the evaluation at the physical point, along with the combined statistical and continuum-extrapolation error.

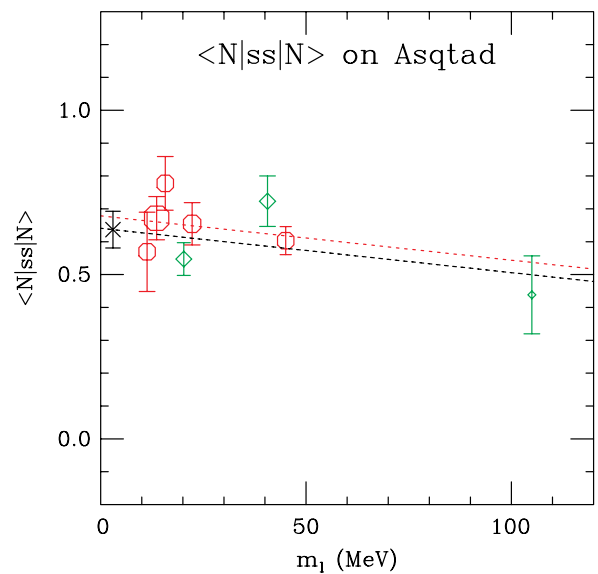


FIG. 9 (color online). $\langle N|\bar{s}s|N\rangle$ on the Asqtad ensembles with the highest statistics, those with at least 1600 configurations, along with the ensemble with $m_l = m_s$ which has a large impact on the chiral extrapolation. Symbols are the same as Fig. 8.

only those ensembles with more than 1600 lattices, along with the ensemble with $m_l = m_s$ which has lower statistics but has a large impact on the slope of the chiral extrapolation.

There are other significant systematic errors. The fit form linear in m_l is of course an approximation, so there is an error due to missing higher-order terms in chiral perturbation theory. The effect of these higher-order terms cannot be reliably determined from the data available. If the chiral fit is modified to include a quadratic term, then the central value changes significantly, but the coefficient of the quadratic term is rather poorly determined and the curvature in the fit is rather extreme; it is unlikely that this curvature represents an actual nonlinearity in the chiral extrapolation, given the analysis of the chiral perturbation theory form given in Sec. IV E. To estimate the systematic error from exclusion of these higher-order terms, we use the case of chiral fits to M_N to estimate the size of the effect from these higher-order terms. If the value of M_N is fit to constant-plus-linear and evaluated at the physical point, the result differs from the result obtained by fitting to two extra orders in M_π by 7%; we thus take 7% as an estimate of the systematic error in $\langle N|\bar{s}s|N\rangle$ due to higher-orders in χ PT. This may be an overly conservative estimate; it is entirely possible that the mass of the nucleon is more sensitive to the masses of the valence quarks than is the nucleon's suppression of the strange quark condensate.

Finite-size effects in general are expected to be small on the MILC Asqtad ensembles, since they have relatively large physical volumes. However, this quantity may be especially sensitive to finite-volume effects. Recall that the physical basis for the nucleon strangeness is that the presence of the nucleon's valence quarks and the glue field holding them together carves out a "bubble" in the QCD vacuum with different characteristics, including the suppression of the strange chiral condensate; since the size of the measured effect is directly related to the size of this region, which could extend over the nucleon and its surrounding pion cloud, it is potentially especially sensitive to small volumes. In general, it is not possible to directly estimate the size of the finite-volume effects. However, in one case, there are two MILC Asqtad ensembles with the same lattice parameters but different physical volumes. One volume corresponds to the volumes used on other ensembles, while one has a spatial extent 40% greater. The measured values of M_N on these ensembles differ by 1%; since it is possible that the nucleon strangeness is more sensitive to finite volume effects, we conservatively estimate the systematic error due to finite volume corrections as 3%. A more direct test of finite size effects is available on the HISQ ensembles, where three ensembles with identical lattice parameters except for the volume are available.

Finally, there is an uncertainty in the values of Z_m used to convert the result from the lattice regularization to the $\overline{\text{MS}}$ (2 GeV) scheme of 4% [30]. The result can be presented in the renormalization-invariant form $m_s\langle N|\bar{s}s|N\rangle$, the strange

TABLE III. Error budget for the measurement of $\langle N|\bar{s}s|N\rangle$ using the (improved) hybrid method on the Asqtad data.

Source	Error
Statistical	0.05
Improved method	0.007
Higher order χ PT	0.05
Excited states	0.03
Finite volume	0.02
Renormalization	0.03

quark sigma term, to eliminate this error. However, in this case there is a systematic error of nearly the same size coming from uncertainty in the physical value of m_s and from uncertainty in lattice scale-setting.

We note that these systematic error estimates correspond to one-standard-deviation uncertainties, suitable for combining in quadrature to obtain an overall error, and not worst-case upper bounds on the systematic effects; it is possible, in the same manner as with the statistical error, that the true deviation from the central value is somewhat larger.

This gives a result, extrapolated to the physical point, of $\langle N|\bar{s}s|N\rangle = 0.637(55)_{\text{stat}}(74)_{\text{sys}}$. The error budget is summarized in Table III. The improvement in the statistical error over that reported in [22] is not as large as was hoped (note that the improved hybrid method reduces statistical error by roughly half); this is due to the lack of improved hybrid results on the finer ensembles due to the expense of recomputing propagators. Thus, the largest remaining contributor to the statistical error is uncertainty in the continuum approximation.

I. Validation from the direct method

The additional measurements made to apply the improved hybrid method are precisely the measurements needed to apply the direct method. Thus, all of the measurements required to implement Eq. (3) have already been made on the coarsest ($a \approx 0.12$ fm) ensembles.

We do not expect the direct method to be competitive with the improved hybrid method for an accurate determination of $\langle N|\bar{s}s|N\rangle$ on these ensembles. It considers less information (fewer $\bar{s}s$ condensate measurements and fewer propagator lengths), and does not explicitly consider the effect of excited states in the nucleon propagator. In particular, it does not consider the alternating-parity state which appears in propagators using staggered fermions. However, it is the preferred method of many other groups calculating the nucleon strangeness, and thus it is appropriate to apply it to the MILC Asqtad data where possible to provide a comparison between the methods. Since we are using it only as a comparison to the (improved) hybrid method and not as a stand alone calculation of the nucleon strangeness, we do not convert to the $\overline{\text{MS}}$ (2 GeV)

regularization scheme or apply corrections for the strange quark mass.

The direct method requires two choices: the length of the propagator (T) and the location within that propagator (T_1 , measured here from the source) where the condensate is evaluated. As usual, there is a systematic/statistical error tradeoff. If the condensate measurement is chosen too close to either end of the propagator, then there is the possibility of contamination by excited states; only far from the source and sink does the propagating state approximate a pure nucleon. If the propagator is chosen to be too short, then nowhere between source and sink is this condition true, and any result will potentially suffer from large systematic error. However, the signal-to-noise ratio of the propagator declines exponentially with increasing distance, so choosing longer propagators leads to larger statistical error.

Figure 10 shows the result for $\langle N|\bar{s}s|N\rangle$ as a function of the location of the $\bar{s}s$ measurement (the value T_1 in Eq. (3)) for a propagator length of $10a$, averaged over the five $a \approx 0.12$ ensembles where the needed measurements have been made. As expected, the result depends strongly on the choice of T_1 ; the most accurate values will be located far from both source and sink. While the length of the propagator is too short to definitively say that a plateau exists, there is certainly the suggestion of one in the region $2a \leq T_1 \leq 5a$. This plateau agrees well with the calculation using the improved hybrid method, reinforcing the validity of that result.

Another very notable feature of this figure is the strong asymmetry between source and sink ends; the result is

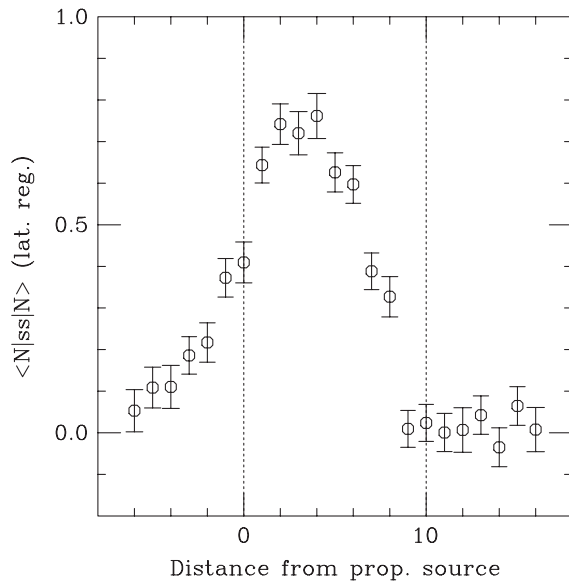


FIG. 10. The intrinsic strangeness of the nucleon on the MILC Asqtad ensembles using the direct method with a propagator length of $10a$, as a function of $\bar{s}s$ insertion time T_1 . Vertical dashed lines represent the sink for the propagator, while the horizontal lines show the average using the improved hybrid method with the “conservative” padding choice.

nearly to its plateau value at the source but consistent with zero at the sink. This is due to the asymmetry of the operators used by MILC to calculate the nucleon two-point function (Coulomb wall source, point sink). Similar asymmetry is notable in Fig. 5, which hints that it would be possibly useful to explore an asymmetric padding window in the improved hybrid method. This effect was also noted by the JLQCD collaboration in their application of the direct method [24] using asymmetric operators.

We can also vary the propagator length used. Figure 11 shows similar curves to Fig. 10 for various length propagators. As expected, longer propagators have higher statistical error (since the propagators themselves are noisier), but the height of the plateau itself increases with increasing propagator length. This is not entirely unexpected, since all of the curves show suppression near the source and sink, and a longer propagator allows for more distance from both. For a result unpolluted by excited states, we should choose a propagator length T long enough that the result as a function of T reaches a plateau; for these ensembles, this appears to be the case for $T \approx 12a$. However, these results are far too noisy to be able to draw much of a conclusion other than that these results appear consistent with those obtained from the improved hybrid method.

It is also possible and beneficial to use multiple condensate time slices and multiple propagator lengths to reduce statistical error. This has a side benefit when applied to a

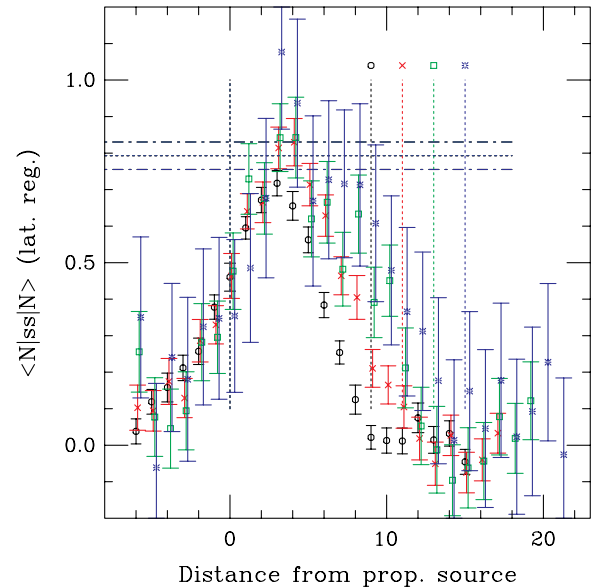


FIG. 11 (color online). The intrinsic strangeness of the nucleon on the MILC Asqtad ensembles using the direct method for multiple propagator lengths, as a function of $\bar{s}s$ insertion time T_1 . Vertical dashed lines represent the source and sink for the various propagators, with the symbol used to indicate the result using that propagator length indicated above the sink. The horizontal lines show the average using the improved hybrid method on these ensembles with the “conservative” padding choice.

calculation like the present one that uses staggered fermions. The interpolating operators used to create and annihilate the nucleon also overlap with states with negative parity whose propagators come with a factor of $(-1)^T$. In particular, the overlap amplitude with the lowest-lying alternating state is often larger than that of the nucleon itself. In the hybrid method, this state is included explicitly in the fit forms used to determine M_N ; however, the direct method offers no such mechanism. Telltale oscillatory behavior is visible, for instance, in the $T = 11$ data in Fig. 11.

While these states have masses greater than that of the nucleon and thus will become irrelevant for condensate measurements taken from sufficiently long propagators at points sufficiently far from source and sink, their influence can be significant for the propagator lengths accessible in the current data set. The splitting between these states and the nucleon is generally less than the splitting with the lowest-lying positive parity excited state, so it will cause a more substantial pollution of the result. This influence can appear in two places: either as an alternating trend in the value of $\langle N|\bar{s}s|N\rangle$ as a function of the location T_1 of the condensate measurement, or as a function of the length T of the propagator used. Figure 11 shows some evidence for this phenomenon.

To reduce the influence of these alternating states, and to reduce statistical error by making use of more of the available data, it is useful to consider the condensate on two (or more) adjacent time slices, and to consider two adjacent propagator lengths. While this does not ensure that there will be no influence from the neglected oscillating staggered-fermion state, it should reduce it, while simultaneously improving the statistics.

Figure 12 shows the resulting values for $\langle N|\bar{s}s|N\rangle$ from the direct method, averaging over two adjacent propagator lengths and considering the strange quark condensate on multiple time slices. The result using the improved hybrid method is shown for comparison. While there is no definitive plateau from which an authoritative value can be taken, the peak values (corresponding to condensate measurements intermediate between source and sink) agree quite well with those from the improved hybrid method.

These results are not conclusive enough to give a quotable result for $\langle N|\bar{s}s|N\rangle$. However, there is strong agreement between the direct and improved hybrid methods on this set of ensembles. As the direct method has been favored by most other recent high-quality calculations of this quantity, its use provides a useful comparison with those results, and its agreement with the hybrid methods (which are admittedly somewhat convoluted) lends strong support to their validity.

J. Validation from the spectrum method

As discussed previously, the spectrum method cannot be used to produce a reliable calculation of $\langle N|\bar{s}s|N\rangle$ using the MILC Asqtad data. The main difficulty is the tendency to

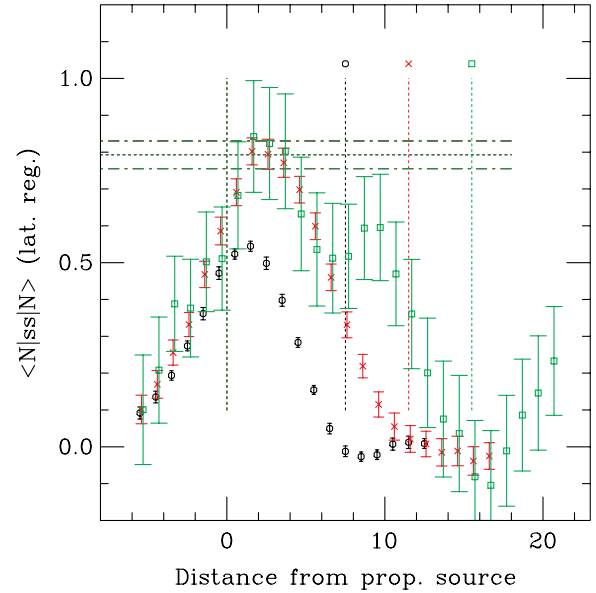


FIG. 12 (color online). Results for the nucleon strangeness $\langle N|\bar{s}s|N\rangle$ from the direct method. The results are averaged over four adjacent condensate measurements at locations centered on the value of t_1 shown, and averaged over two adjacent propagator lengths. The intrinsic strangeness of the nucleon on the MILC Asqtad ensembles using the direct method for multiple propagator lengths, as a function of $\bar{s}s$ insertion time T_1 . The results are averaged over four adjacent condensate measurements at locations centered on the value of t_1 shown, and averaged over two adjacent propagator lengths. Dotted vertical lines indicate the source and sink locations, with the sink position shown equidistant between the sinks of the two adjacent propagators that are averaged. Symbols above these dotted lines indicate the plot symbols corresponding to that propagator length. The horizontal lines show the average using the improved hybrid method on these ensembles with the “conservative” padding choice.

change β between ensembles to keep the lattice spacing, defined via a Sommer scale [33] and thus dependent on m_l , constant.

However, in the event that several ensembles are available with different quark masses but the same β and other lattice parameters (i.e. the lattice size and tadpole improvement factor u_0), then some information can be gleaned from calculating M_N on them. There is only one instance in the Asqtad library where two ensembles have the same β and different m_s (and m_l). Due to a mistake in lattice generation, two ensembles were run with $\beta = 7.10$. The first has $am_l = 0.0093$, $am_s = 0.031$, and the second has $am_l = 0.0062$, $am_s = 0.0186$. These ensembles both have the same dimension ($28^3 \times 96$) and tadpole factor $u_0 = 0.8785$.

This comparison is made more complicated by the fact that these ensembles differ in both the light and strange quark masses. Thus, we cannot independently determine $\frac{\partial M_N}{\partial m_s}$ or $\frac{\partial M_N}{\partial m_l}$, only a linear combination of the two.

Nonetheless, this provides sufficient information to compare with the larger result from the hybrid method.

Referring to these ensembles as A and B and applying the Feynman-Hellman theorem, we should have

$$M_{N,A} - M_{N,B} = (0.0093 - 0.0062) \left(\frac{\partial M_N}{\partial m_{l,sea}} + \frac{\partial M_N}{\partial m_{l,val}} \right) + (0.031 - 0.0186) \frac{\partial M_N}{\partial m_s}. \quad (12)$$

Since $\frac{\partial M_N}{\partial m_{l,sea}} = 2\langle N|\bar{u}u|N\rangle_{disc}$ and $\frac{\partial M_N}{\partial m_s} = \langle N|\bar{s}s|N\rangle$, both of which have been calculated using the improved hybrid method, this suggests a constraint on $M_{N,A} - M_{N,B}$. However, we have no such estimate for $\frac{\partial M_N}{\partial m_{l,val}}$. To eliminate this contribution, we have calculated partially quenched propagators on the $am_l = 0.0093$, $am_s = 0.031$ ensemble with $am_{val} = 0.0062$, giving the masses of two nucleons with the same valence quark mass that differ only in their sea quark masses. Partially quenched propagators were run on only 1020 configurations out of the 1137 equilibrated configurations in the ensemble; the $am_l = 0.0062$, $am_s = 0.0186$ ensemble has 948 configurations.

Referring to the former mass as $M_{N,A'}$, we have

$$M_{N,A'} - M_{N,B} = 2(0.0093 - 0.0062)\langle N|\bar{u}u|N\rangle_{disc} + (0.031 - 0.0186)\langle N|\bar{s}s|N\rangle \quad (13)$$

where the values of $\langle N|\bar{u}u|N\rangle$ and $\langle N|\bar{s}s|N\rangle$ should be evaluated not at the physical point but at quark masses

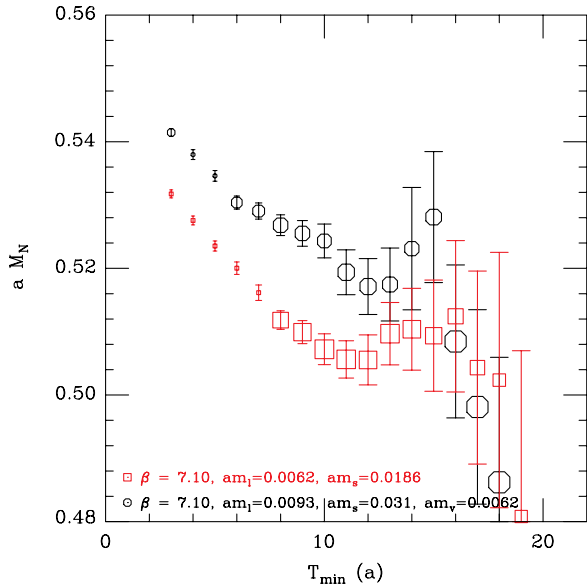


FIG. 13 (color online). Results for M_N on the two ensembles with $\beta = 7.10$, $am_l = 0.0093$, $am_s = 0.031$, $am_{val} = 0.0062$ (black octagons) and $\beta = 7.10$, $am_l = 0.0062$, $am_s = 0.0186$ (red squares), at varying values of T_{min} , using a two-state fit method. Symbol size indicates fit quality. Absent data indicate fits that failed to converge or converged to nonsensical values.

TABLE IV. Results for heavy and light quark content of the nucleon on $\beta = 7.10$, $am_l = 0.0093$, $am_s = 0.031$ and $\beta = 7.10$, $am_l = 0.0062$, $am_s = 0.0186$ ensembles, and a weighted average.

Ensemble	$\langle N \bar{s}s N\rangle$	$\langle N \bar{u}u N\rangle$
$am_l = 0.0093$, $am_s = 0.031$	1.09(18)	1.75(28)
$am_l = 0.0062$, $am_s = 0.0186$	0.77(22)	0.53(36)
Weighted average	0.96(14)	1.29(22)

intermediate between ensembles A and B, and the factor of two is due to the presence of two degenerate light quark flavors in the sea.

Figure 13 shows the result of a two-state fit to the nucleon propagator on these two ensembles as a function of the minimum fit distance.

On both ensembles, both fits produce the expected plateau starting at around $T_{min} \approx 10$. $T_{min} = 11$ represents the best compromise between statistical error and possible excited-state pollution for determining the difference in M_N ; this gives the values $M_{N,A'} = 0.519(4)$ for the $am_l = 0.0093$, $am_{val} = 0.0062$ ensemble and $M_{N,B} = 0.506(3)$ for the $am_l = 0.0062$ ensemble. Combining the errors in quadrature, we get $M_{N,A'} - M_{N,B} = 0.013(5)$.

To test this against the hybrid method, we calculate $(0.0093 - 0.0062)\langle N|\bar{u}u|N\rangle + (0.031 - 0.0186)\langle N|\bar{s}s|N\rangle$ which should give a similar result. First, it is simplest to average the values of $\langle N|\bar{u}u|N\rangle$ and $\langle N|\bar{s}s|N\rangle$ on these two ensembles. Results from the hybrid method with $T_{min} = 7$ are given in Table IV.

Note that ensemble B has $\langle N|\bar{s}s|N\rangle < \langle N|\bar{u}u|N\rangle$, which is unexpected; this difference, however, is not statistically significant ($\langle N|\bar{s}s|N\rangle - \langle N|\bar{u}u|N\rangle = 0.24(28)$, with the error bar computed in the proper way via jackknife).

These values give $(0.0093 - 0.0062)\langle N|\bar{u}u|N\rangle + (0.031 - 0.0186)\langle N|\bar{s}s|N\rangle = 0.011(4)$, in reasonable agreement with the $0.013(5)$ estimated from the difference of the nucleon masses. This agreement between the hybrid and spectrum methods on these two ensembles lends support to the validity of the former.

V. $\langle N|\bar{s}s|N\rangle$ FROM THE MILC HISQ DATA

The hybrid method can also be applied to the newer HISQ data with no significant modification, although none of the measurements required to apply the improved hybrid method are available. Several features of the HISQ data set make it somewhat less suitable for analysis. There is a more limited range of light quark masses available, ranging from the physical value to $0.2m_s$. This greatly reduces the “lever arm” available to determine the slope of the chiral extrapolation compared to the Asqtad ensembles, where each nominal lattice spacing had runs with $m_l = 0.4m_s$,

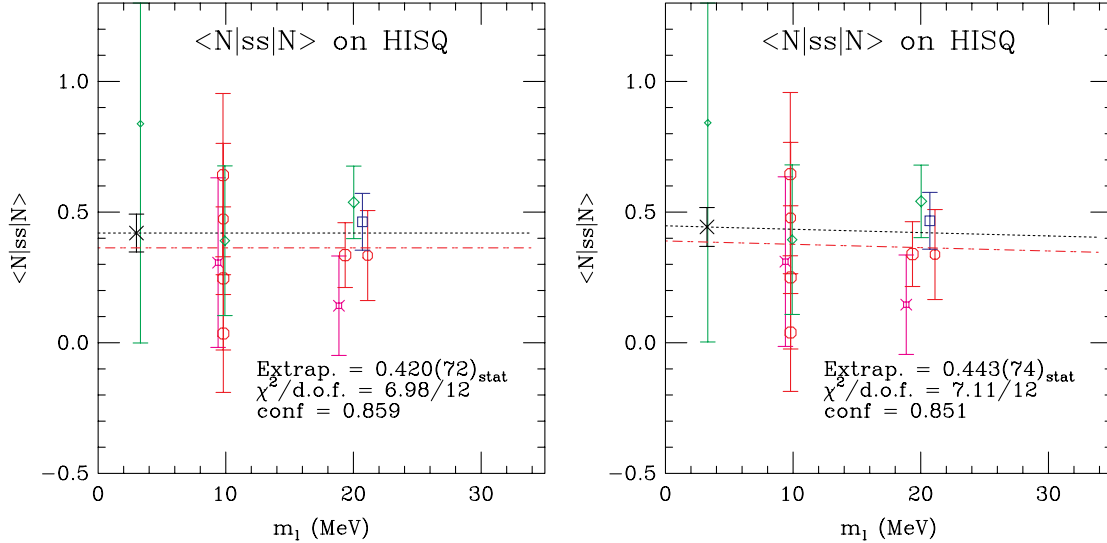


FIG. 14 (color online). The intrinsic strangeness of the nucleon on the MILC HISQ ensembles, using the hybrid method. The left pane shows a constant fit; the right pane shows a linear chiral fit, with the slope constrained using a Bayesian prior from the Asqtad fit. Ensembles with $a \approx (0.15, 0.12, 0.09, 0.06)$ fm are shown as violet fancy squares, red octagons, green diamonds, and blue squares, respectively. Symbol area is proportional to the number of gauge configurations in the ensemble. The fit at the continuum is shown as a black dotted line, while the fit evaluated at $a = 0.12$ fm is shown as a red dashed line. The fit evaluated at the continuum is shown as a black cross, and the quoted error includes the uncertainty in the continuum extrapolation with the prior as discussed in the text.

and one ensemble with $a \approx 0.09$ fm has $m_l = m_s$ (three degenerate heavy quarks). The HISQ ensembles are all limited to 1000 equilibrated gauge configurations, and the gauge generation program is still ongoing, limiting the statistics available.

Nonetheless, essentially the same analysis can be carried out. The form of the chiral and continuum extrapolations will be unchanged, although the value of the constant controlling the continuum extrapolation should be smaller since taste breaking, the dominant discretization error in the Asqtad action, is reduced roughly by two-thirds in HISQ. Since the continuum extrapolation does not have much of an effect, we keep the prior with a width corresponding to a 10% discretization effect from $a = 0.12$ fm to the continuum; while this effect should be reduced in HISQ, we have no basis for estimating to what extent that is the case. The values of Z_m to convert to the $\overline{\text{MS}}$ (2 GeV) regularization are, to sufficient accuracy, the same for HISQ and Asqtad.

TABLE V. Error budget for the measurement of $\langle N|\bar{s}s|N\rangle$ using the unimproved hybrid method on the HISQ data.

Source	Error
Statistical	0.08
Higher order χ PT	0.03
Excited states	0.02
Finite volume	0.01
Renormalization	0.03

The same minimum distance to consider for the nucleon fits in order to avoid excited state pollution is also still sensible; nothing in the physics which controls excited state pollution is affected by the further improved fermion action.

Applying the same analysis described in detail previously, we obtain nonsensical results due to the lack of sufficient lever arm to constrain the slope of the chiral extrapolation, due to the lack of ensembles with heavier light quarks. While we may omit the m_l dependence from the fit, a somewhat more sophisticated approach is to constrain the slope of the chiral fit. We use a Gaussian Bayesian prior whose central value is taken from the Asqtad fit and whose width is equal to the error of the Asqtad slope. The constant fit and the fit with a constrained slope are shown in Fig. 14.

These two fits are very similar; we consider the fit with the constrained slope to be more physical.

The systematic errors should be similar to those in the Asqtad case. Since the HISQ ensembles have larger physical volumes, we use 2% as an estimate of the systematic error from finite-volume effects. The error budget is summarized in Table V.

Thus, our result extrapolated to the physical point is $\langle N|\bar{s}s|N\rangle = 0.44(8)_{\text{stat}}(5)_{\text{sys}}$.

VI. $\langle N|\bar{c}c|N\rangle$ FROM THE MILC HISQ DATA

The intrinsic charm of the nucleon can also be measured on the lattice. This is interesting both in its own right and because it can be compared with the perturbative

prediction. Since the lattice calculation directly measures $\langle N|\bar{c}c|N\rangle$, we convert Kryjevski's perturbative computation [23] to this form. Using $x_{uds} = 0.14$ and $m_c = 1.2$ GeV, the perturbative prediction is $\langle N|\bar{c}c|N\rangle = 0.057$. Due to the smaller absolute magnitude of the intrinsic charm, and the lower statistics of the HISQ ensembles used to determine it, it is even more difficult to extract than the nucleon strangeness.

A. The lattice result

The application of the hybrid method to the nucleon intrinsic charm proceeds identically to the nucleon strangeness, except that the charm quark condensate is used. Pollution due to excited states should have a similar impact on the intrinsic charm and the intrinsic strangeness, so for a first analysis we use the same set of minimum fit distances for M_N as before. The results on the various HISQ ensembles are shown in Fig. 15, along with the fit. The results are broadly consistent with the perturbative prediction, but indistinguishable from zero due to the large fractional statistical errors. We thus do not attempt a chiral extrapolation. For the continuum extrapolation, we use the same procedure as for the nucleon strangeness, by adding a term proportional to a^2 to the fit. Since the coefficient of such a term would be extremely poorly determined given the high statistical errors, we use the same procedure as before to constrain it (see Sec. IV G) by the imposition of a Bayesian prior with a width corresponding to a 10% effect between $a = 0.12$ fm and the continuum. (Note however that as the 10% figure

was obtained from Asqtad lattices, smaller lattice discretization effects might be expected on HISQ if these effects stem from taste-breaking interactions.) This difference is not terribly meaningful, of course, given the size of the statistical errors involved. However, in this case the fit value of the nucleon intrinsic charm is very nearly zero, so the allowance for a 10% effect would lead to an artificially tight prior. Thus, we impose a prior that allows for an 0.02 shift between $a = 0.12$ fm and the continuum, which is roughly 1/3 the perturbative prediction. (In practice, the width of this prior has essentially no effect on such a noisy fit.)

Recall that the choice of the minimum propagator length t_{\min} used to fit the nucleon propagator was made to provide the best available balance between the statistical error (reduced for lower values of t_{\min}) and the potential for systematic error due to excited-state pollution (larger at lower values of t_{\min}). The balance between these two errors struck for the nucleon strangeness was appropriate for a quantity with smaller statistical errors, but when dealing with the nucleon charm the impact of additional excited state pollution is not as meaningful when dealing with a quantity with such a large statistical error. Additionally, per the perturbative argument [29,23], excited-state pollution should matter less when dealing with heavy quarks, since the effect of altering the mass of a quark well above the scale Λ_{QCD} affects all low-energy quantities (i.e. the masses of the nucleon and its excited states) in the same way, interpreted as an overall rescaling of the lattice. This is not strictly true, of course, since the charm quark is not that much greater in mass than Λ_{QCD} ; otherwise, the

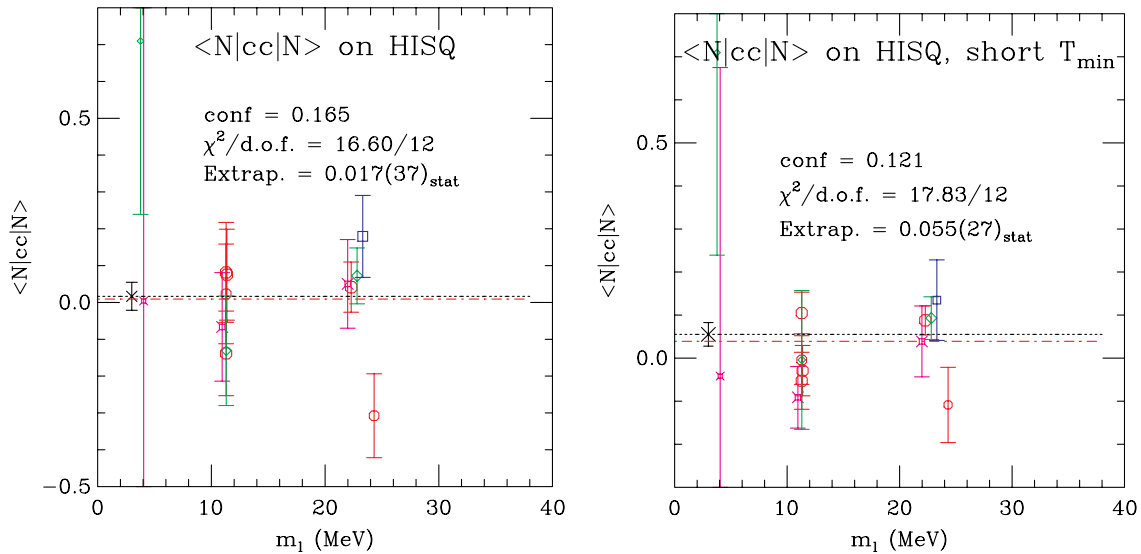


FIG. 15 (color online). The intrinsic charm content of the nucleon on the MILC HISQ ensembles using the hybrid method. The left pane shows the result using the larger minimum propagator distances t_{\min} used for the strangeness calculation; the right pane shows the result using the smaller minimum propagator distances discussed in the text. Ensembles with $a \approx (0.15, 0.12, 0.09, 0.06)$ fm are shown as violet fancy squares, red octagons, green diamonds, and blue squares, respectively. Symbol area is proportional to the number of gauge configurations in the ensemble. The fit at the continuum is shown as a black dotted line, while the fit evaluated at $a = 0.12$ fm is shown as a red dashed line. The fit evaluated at the continuum is shown as a black cross, and the quoted error includes the uncertainty in the continuum extrapolation with the prior as discussed in the text.

inclusion of dynamical charm in simulations of low-energy quantities would be meaningless, since by the same argument all they would do is change the lattice spacing. Nonetheless, it suggests that the effect due to excited state pollution is less for the intrinsic charm than for the strangeness.

It is thus appropriate to use smaller minimum distances in evaluating the nucleon intrinsic charm. As before, we should choose a minimum distance that is relatively constant in physical units across lattice spacings. No methodical evaluation of the systematic errors due to excited state pollution can really be made with these data, so we choose (in a rather *ad hoc* way) to use minimum distances that are roughly $2/3$ those used for the strangeness. (A somewhat artificial lower bound on the minimum distances used, especially for the coarser ensembles, is provided by fitter convergence; if there is too much excited state pollution, the nucleon mass fits may behave unpredictably.) We thus choose $t_{\min} = (3a, 3a, 5a, 7a)$ for the $a \approx (0.15, 0.12, 0.09, 0.06)$ fm ensembles, respectively.

Using the same minimum distances that were used in for $\langle N | s \bar{s} | N \rangle$, ($10a$ for $a \approx 0.06$ fm, $7a$ for $a \approx 0.09$ fm, $5a$ for $a \approx 0.12$ fm, and $4a$ for $a \approx 0.15$ fm), we would find that $\langle N | \bar{c} c | N \rangle = 0.017(37)_{\text{stat}}$. Using the smaller minimum distances discussed above, we obtain $\langle N | \bar{c} c | N \rangle = 0.056(27)_{\text{stat}}$ if the coarsest ensembles are included, and $\langle N | \bar{c} c | N \rangle = 0.054(27)_{\text{stat}}$ if they are omitted. This result has, as expected, lower statistical error, in agreement with the perturbative prediction [23]. We make no estimates of systematic errors because of the large size of the statistical uncertainty. These values are broadly consistent with the perturbative predictions given by Kryjevski [23].

VII. CONCLUSIONS

Early lattice work on the nucleon strangeness was prompted in part by early χ PT calculations suggesting that its value might be large [3], and thus provide a significant enhancement to the WIMP-on-baryon scattering cross-section. While there is no reason to expect the perturbative method in Refs. [29,23] to apply accurately to the strange quark, that result can be used to set a natural scale for $\frac{\partial M_N}{\partial m_s} \approx \frac{2}{29} \frac{M_N}{m_s} \approx 0.7$. Early lattice calculations suffered from large uncontrolled systematics, leading to wildly varying estimates for the nucleon strangeness, some of which were large. This work, as well as our previous work on the nucleon strangeness in Ref. [22] and many other recent calculations [9–12], however, all conclude that the nucleon strangeness is approximately at its natural scale, substantially smaller than the early work suggested that it might be. While the uncertainty in the value of $\langle N | \bar{s} s | N \rangle$ is still large compared to other lattice quantities, it is no longer a dominant contribution to the uncertainty in dark matter scattering amplitudes; from the perspective of direct dark matter detection experiments, the problem presented in Refs. [1,2], of whether the nucleon strangeness is

“small” or “large” has been answered in favor of the former. In fact, the contribution to the dark matter scattering cross section from strange quark loops in the nucleon, coming from diagrams of the type shown in Fig. 1, is actually smaller than that from the heavy quarks for which the perturbative method is valid.

We apply the “hybrid method,” outlined in Sec. III C, to the large library of improved staggered gauge configurations (roughly 26000 Asqtad and 14000 HISQ) generated by the MILC Collaboration. Improved staggered fermions are well suited to this project, since they are very fast, allowing for large gauge ensembles with which to beat down the inherently noisy disconnected diagrams involved here, and they preserve a remnant chiral symmetry, allowing for a straightforward application of the Feynman-Hellman theorem without the concerns about additive renormalization or operator mixing which plague Wilson-based computations of this quantity, as discussed in Ref. [7].

We present an improvement on this method which, due to historical averaging over sources and time slices when measuring $\bar{q}q$ and the nucleon propagator, required repeating the lattice measurements of these quantities; this was thus only performed on the coarser lattices in the Asqtad library (some 14000 configurations out of 26000 total) to economize on computer time. We determine that the condensate should be considered out to a distance of approximately 0.7 fm from the source and sink of the nucleon propagator. This results in an approximately 40–50% decrease in the statistical error.

Using the improved hybrid method where the needed measurements are available, we conclude that $\langle N | \bar{s} s | N \rangle = 0.637(55)_{\text{stat}}(74)_{\text{sys}}$ after continuum and chiral extrapolation. The leading uncertainties are statistical, mainly in the continuum extrapolation, and in the systematic error due to excited state contamination. Since smaller statistical errors allow the use of larger minimum distances (to reduce excited state errors) or allow the justification of smaller systematic error estimates for the minimum distances chosen, improvements in statistics will also lead to improvements in this systematic error. Availability of the needed measurements to apply the improved hybrid method on more of the finer ensembles would help with this, as well as helping to reduce the large contribution to the statistical error from the continuum extrapolation. We note that the systematic errors quoted here represent one-standard-deviation uncertainties rather than worst-case upper bounds on the size of the systematic effects, as the aim in estimating them is to construct estimates which can be combined in quadrature with each other and with the statistical error in the normal way; it is possible that the true size of the systematic effects may be larger.

This method can also be used to calculate the nucleon strangeness using the HISQ fermion action. Due to the lack of large- m_l ensembles in the HISQ program, we constrain

the slope of the chiral extrapolation using a Gaussian Bayesian prior whose central value and width are taken from the Asqtad fit. We obtain $\langle N|\bar{s}s|N\rangle = 0.437(8)_{\text{stat}}(5)_{\text{sys}}$.

The same methods can be used to compute the intrinsic charm of the nucleon. This provides a connection to perturbative QCD. A simple argument involving the running of the QCD coupling constant and the fact that the low-energy QCD scale is set by the running of g can be used to estimate $\langle N|\bar{c}c|N\rangle$ [3,29]; that result has been improved to four-loop order by Kryjevski [23], who calculates $\langle N|\bar{c}c|N\rangle = 0.058$.

Using the MILC HISQ ensembles with dynamical charm, we apply similar methods as with the intrinsic strangeness. Excited-state pollution is less of a problem for this quantity; by Kryjevski's perturbative argument, the effect of altering the charm quark mass mostly just rescales the lattice, so the intrinsic charm of the excited states of the nucleon interpolating operator should be similar to that of the ground state. Moreover, we are dealing with fractional statistical errors that are about an order of magnitude larger. Thus, we choose smaller minimum propagator fit distances T_{min} to improve the statistics. Similarly, because the overall statistical error is so high, we do not attempt a chiral extrapolation.

Doing the continuum fit in the same manner as before, we obtain $\langle N|\bar{c}c|N\rangle = 0.056(27)_{\text{stat}}$, essentially the same as the perturbative result albeit with large fractional error due to the lower value. As this error is dominated by statistics, we do not present a systematic error budget. This result can be improved by the simple availability of more HISQ data, as the MILC HISQ lattice generation project progresses.

Taken together, these results for the scalar strange and charm quark content of the nucleon, similar results for the strange quark content from other groups (Fig. 2), and the

perturbative calculation, lead to the amusing conclusion that the scattering of a low-momentum Higgs particle (as in dark matter interactions in the MSSM) is not dominated by the strange quarks in the nucleon, but instead receives more or less equal contributions from all heavy quarks.

ACKNOWLEDGMENTS

This work was supported by the Department of Energy Grants No. DE-FG02-04ER-41298 and No. DE-FG02-95ER-40907. Computer time was provided through the National Energy Resources Supercomputing Center (NERSC), which is supported by the Office of Science of the U.S. Department of Energy under Contract No. DE-AC02-05CH11231. Computer resources were also provided by the USQCD Collaboration, the Argonne Leadership Computing Facility, and the Los Alamos National Laboratory Computing Center, which are funded by the U.S. Department of Energy. Computer resources were also provided by the National Science Foundation's NRAC, Teragrid and XSEDE programs, including the National Center for Supercomputing Applications (NCSA), the Texas Advanced Computing Center (TACC), the Pittsburgh Computer Center (PSC), the National Institute for Computational Sciences (NICS), and the San Diego Supercomputer Center (SDSC). Computer time at the National Center for Atmospheric Research was provided by NSF MRI Grant No. CNS-0421498, NSF MRI Grant No. CNS-0420873, NSF MRI Grant No. CNS-0420985, NSF sponsorship of the National Center for Atmospheric Research, the University of Colorado, and a grant from the IBM Shared University Research (SUR) program. We thank David Kaplan, Ulf Meissner, Michael Engelhardt, and our MILC collaboration colleagues for helpful discussions and suggestions.

-
- [1] E. A. Baltz, M. Battaglia, M. E. Peskin, and T. Wizansky, *Phys. Rev. D* **74**, 103521 (2006).
 - [2] J. Ellis, K. Olive, and C. Savage, *Phys. Rev. D* **77**, 065026 (2008).
 - [3] A. Nelson and D. Kaplan, *Phys. Lett. B* **192**, 193 (1987); D. B. Kaplan and A. Manohar, *Nucl. Phys.* **B310**, 527 (1988).
 - [4] M. Fukugita, Y. Kuramashi, M. Okawa, and A. Ukawa, *Phys. Rev. D* **51**, 5319 (1995).
 - [5] S. J. Dong, J.-F. Lagaë, and K.-F. Liu, *Phys. Rev. D* **54**, 5496 (1996).
 - [6] S. Güsken, P. Ueberholz, J. Viehoff, N. Eicker, P. Lacock, T. Lippert, K. Schilling, A. Spitz, and T. Struckmann (SESAM Collaboration), *Phys. Rev. D* **59**, 054504 (1999).
 - [7] C. Michael, C. McNeile, and D. Hepburn (UKQCD Collaboration), *Nucl. Phys. B, Proc. Suppl.* **106–107**, 293 (2002).
 - [8] G. Bali, S. Collins, and A. Schäfer, *Proc. Sci., LATTICE2008* (2008) 161 [arXiv:0811.0807v2].
 - [9] H. Ohki, H. Fukaya, S. Hashimoto, T. Kaneko, H. Matsufuru, J. Noaki, T. Onogi, E. Shintani, and N. Yamada (JLQCD Collaboration), *Phys. Rev. D* **78**, 054502 (2008).
 - [10] H. Ohki *et al.* (JLQCD Collaboration), *Proc. Sci., LAT2009* (2009) 124 [arXiv:0910.3271].
 - [11] K. Takeda, T. Onogi, S. Aoki, S. Hashimoto, T. Kaneko, and N. Yamada (JLQCD Collaboration), *Proc. Sci., Lattice 2010* (2010) 160.
 - [12] M. Engelhardt, *Proc. Sci., Lattice 2010* (2010) 137 [arXiv:1011.6058].
 - [13] S. Dürr *et al.*, *Phys. Rev. D* **85**, 014509 (2012).
 - [14] R. Horsley, Y. Nakamura, H. Perlt, D. Pleiter, P. E. L. Rakow, G. Schierholz, A. Schiller, H. Stüben, F. Winter,

- and J. M. Zanotti (QCDSF-UKQCD Collaboration), *Phys. Rev. D* **85**, 034506 (2012).
- [15] G. Bali *et al.*, *Phys. Rev. D* **85**, 054502 (2012).
- [16] S. Dinter, V. Drach, R. Frezzotti, G. Herdoiza, K. Jansen, and G. Rossi, *J. High Energy Phys.* **08** (2012) 037.
- [17] P. Shanahan, A. Thomas, and R. Young, *Phys. Rev. D* **87**, 074503 (2013).
- [18] H. Ohki, K. Takeda, S. Aoki, S. Hashimoto, T. Kaneko, H. Matsufuru, J. Noaki, and T. Onogi (JLQCD Collaboration), *Phys. Rev. D* **87**, 034509 (2013).
- [19] M. Engelhardt, *Phys. Rev. D* **86**, 114510 (2012).
- [20] P. Junnarkar and A. Walker-Loud, *Phys. Rev. D* **87**, 114510 (2013).
- [21] C. Jung (RBC/UKQCD Collaboration) Proc. Sci., Lattice 2012 (2012) 164 [[arXiv:1301.5397](#)].
- [22] D. Toussaint and W. Freeman (MILC Collaboration), *Phys. Rev. Lett.* **103**, 122002 (2009).
- [23] A. Kryjevski, *Phys. Rev. D* **70**, 094028 (2004).
- [24] K. Takeda, S. Aoki, S. Hashimoto, T. Kaneko, J. Noaki, and T. Onogi (JLQCD Collaboration), *Phys. Rev. D* **83**, 114506 (2011).
- [25] R. Babich, R. Brower, M. Clark, G. Fleming, J. Osborn, and C. Rebbi, Proc. Sci., LAT2008 (2008) 160 [[arXiv:0901.4569](#)].
- [26] R. Babich, R.C. Brower, M.A. Clark, G.T. Fleming, J.C. Osborn, C. Rebbi, and D. Schaich, *Phys. Rev. D* **85**, 054510 (2012).
- [27] W. Freeman and D. Toussaint, Proc. Sci., Lattice 2010 (2010) 138 [[arXiv:0912.1144](#)].
- [28] A. Bazavov *et al.* (MILC Collaboration), *Rev. Mod. Phys.* **82**, 1349 (2010).
- [29] M. A. Shifman, A. I. Vainshtein, and V. I. Zakharov, *Phys. Lett.* **78B**, 443 (1978).
- [30] Q. Mason, H. D. Trotter, R. Horgan, C. T. H. Davies, and G. P. Lepage, *Phys. Rev. D* **73**, 114501 (2006).
- [31] M. Frink and U.-G. Meißner, *J. High Energy Phys.* **07** (2004) 028.
- [32] A. Bazavov *et al.*, Proc. Sci., LAT2009 (2009) 079 [[arXiv:0910.3618v2](#)].
- [33] R. Sommer, *Nucl. Phys.* **B411**, 839 (1994).